Supplementary Information

Hepatic Hdac3 promotes gluconeogenesis by repressing lipid synthesis and sequestration

Zheng Sun[1], Russell A. Miller[1], Rajesh T. Patel[1], Jie Chen[3], Ravindra Dhir[1], Hong Wang[4], Dongyan Zhang[5], Mark J. Graham[6], Terry G. Unterman[7], Gerald I. Shulman[5], Carole Sztalryd[4], Michael J. Bennett[2, 3], Rexford S. Ahima[1], Morris J. Birnbaum[1], and Mitchell A. Lazar[1]

[1]Division of Endocrinology, Diabetes, and Metabolism, Department of Medicine, Department of Genetics, and The Institute for Diabetes, Obesity, and Metabolism, Perelman School of Medicine at the University of Pennsylvania, Philadelphia, PA 19104, USA

[2]Department of Pathology and Laboratory Medicine, Perelman School of Medicine at the University of Pennsylvania, Philadelphia, PA 19104, USA

[3]Department of Pathology and Laboratory Medicine, Children's Hospital of Philadelphia, Philadelphia, PA 19104, USA

[4]The Geriatric Research, Education and Clinical Center, Baltimore Veterans Affairs Health Care Center, Division of Endocrinology, Department of Medicine, School of Medicine, University of Maryland, Baltimore, MD 21201

[5]Department of Medicine, Yale University School of Medicine, New Haven, CT 06520, USA

[6]Isis Pharmaceuticals, Inc., Carlsbad, CA 92010, USA

[7]Section of Endocrinology, Diabetes and Metabolism, University of Illinois at Chicago, and Jesse Brown VA Medical Center, Chicago, IL 60612, USA

Address Correspondence to: Mitchell A. Lazar, M.D., Ph.D.
Phone: (215) 898-0198; e-mail: lazar@mail.med.upenn.edu

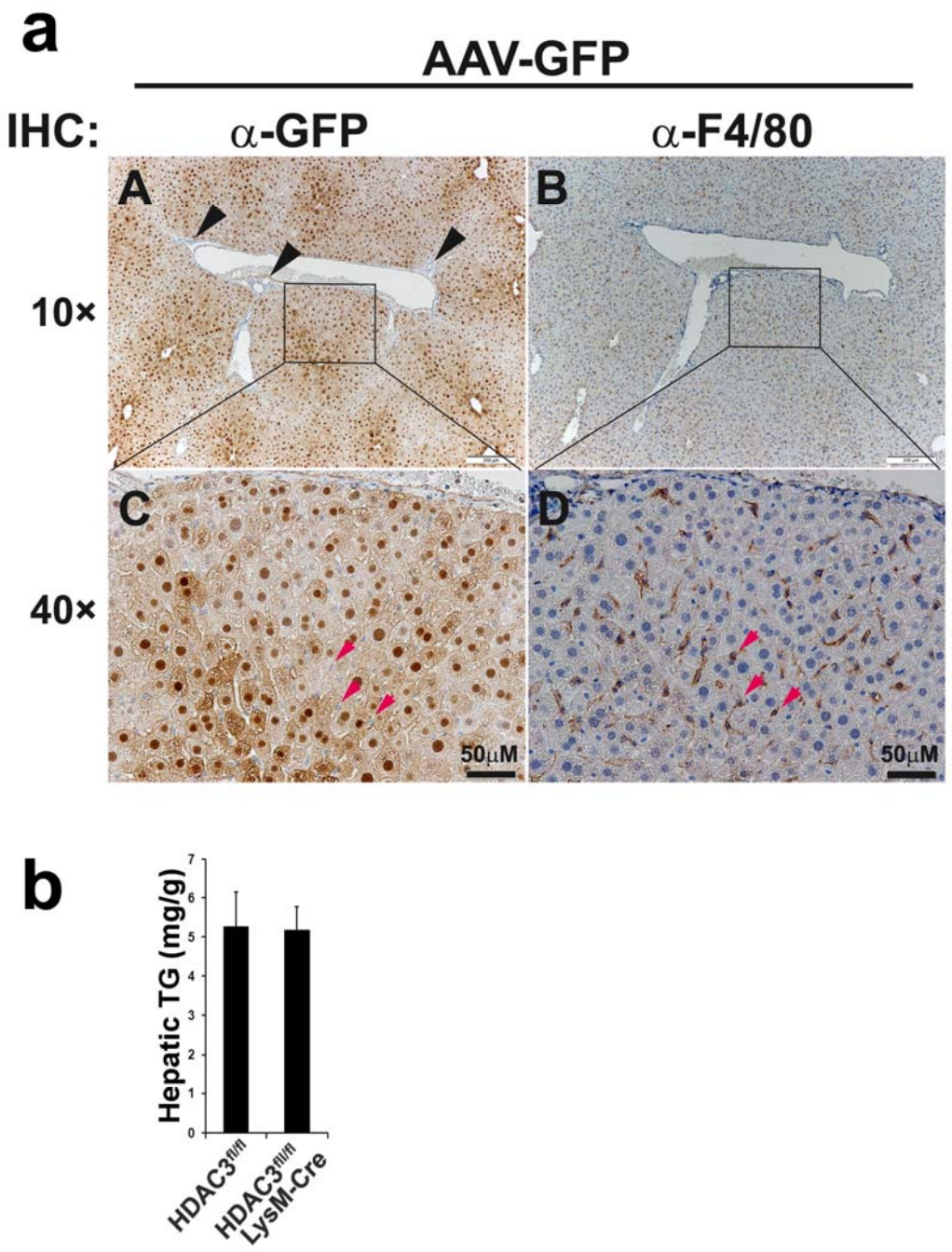

Supplementary Figure 1. The metabolic phenotype observed in Hdac3 liver-specific knockout mice is not confounded by deletion of Hdac3 in Kupffer cells. (**a**) Immunohistochemistry analysis of adjacent paraffin-embedded liver sections from mice injected with AAV-GFP, using the antibody to GFP (α-GFP) and the antibody to Emr1 (α-F4/80) respectively. Note: GFP is not expressed in endothelial cells (black arrows) or F4/80 positive Kupffer cells (pink arrows). (**b**) Hepatic TG measurement on 4-month old *Hdac3*$^{fl/fl}$, LysM-Cre mice. Mice with Hdac3 depleted in all macrophages do not develop fatty liver. $n = 6$. Error bars indicate s.e.m.

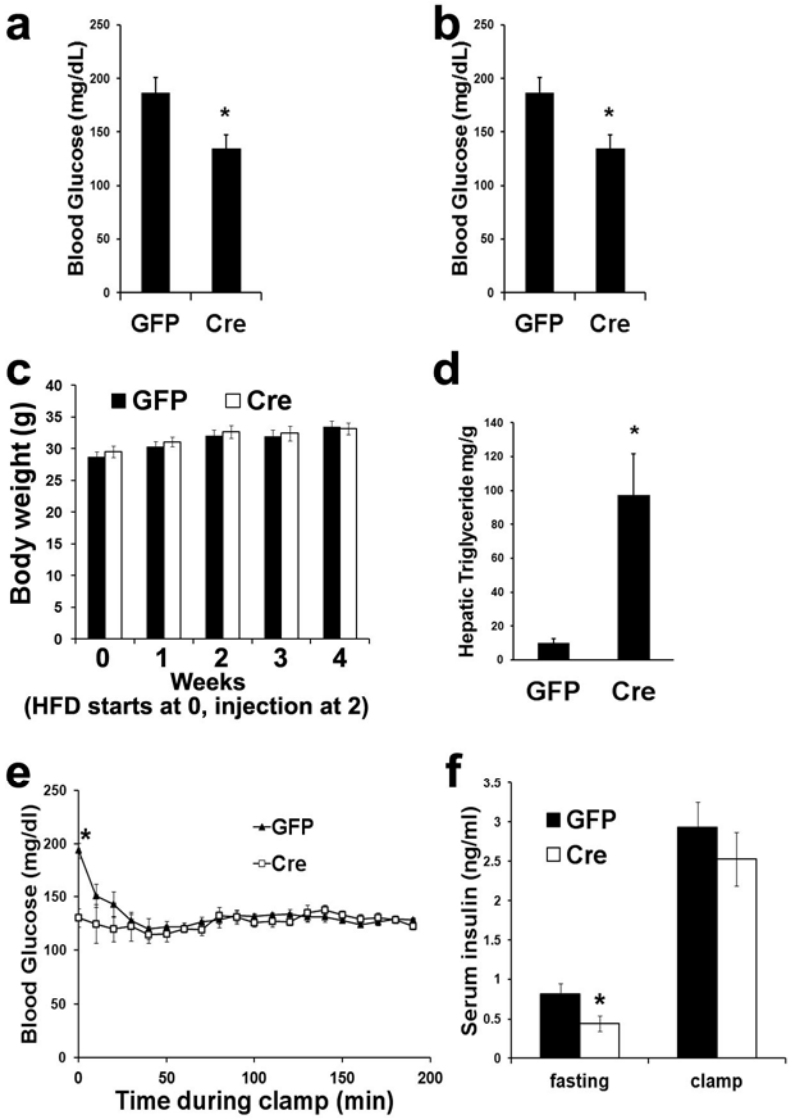

Supplementary Figure 2. Metabolic characterizations of mice without hepatic Hdac3. (**a**) Hepatic TG measurement in 4-month old female mice at 2-weeks after AAV injection, $n = 4$. (**b**) Blood glucose measurement in adult female mice after 6 hr fasting, $n = 4$. (**c**) Body weight mice on high-fat diet (HFD). $n = 8$. (**d**) Hepatic TG measurement at 3-weeks post-injection after feeding HFD for 5 weeks. $n = 8$. (**e**) Blood glucose concentrations during the clamp study. $n = 5–6$. (**f**) Serum insulin concentrations before and after clamp. $n = 5–6$. Error bars indicate s.e.m. * $P < 0.05$.

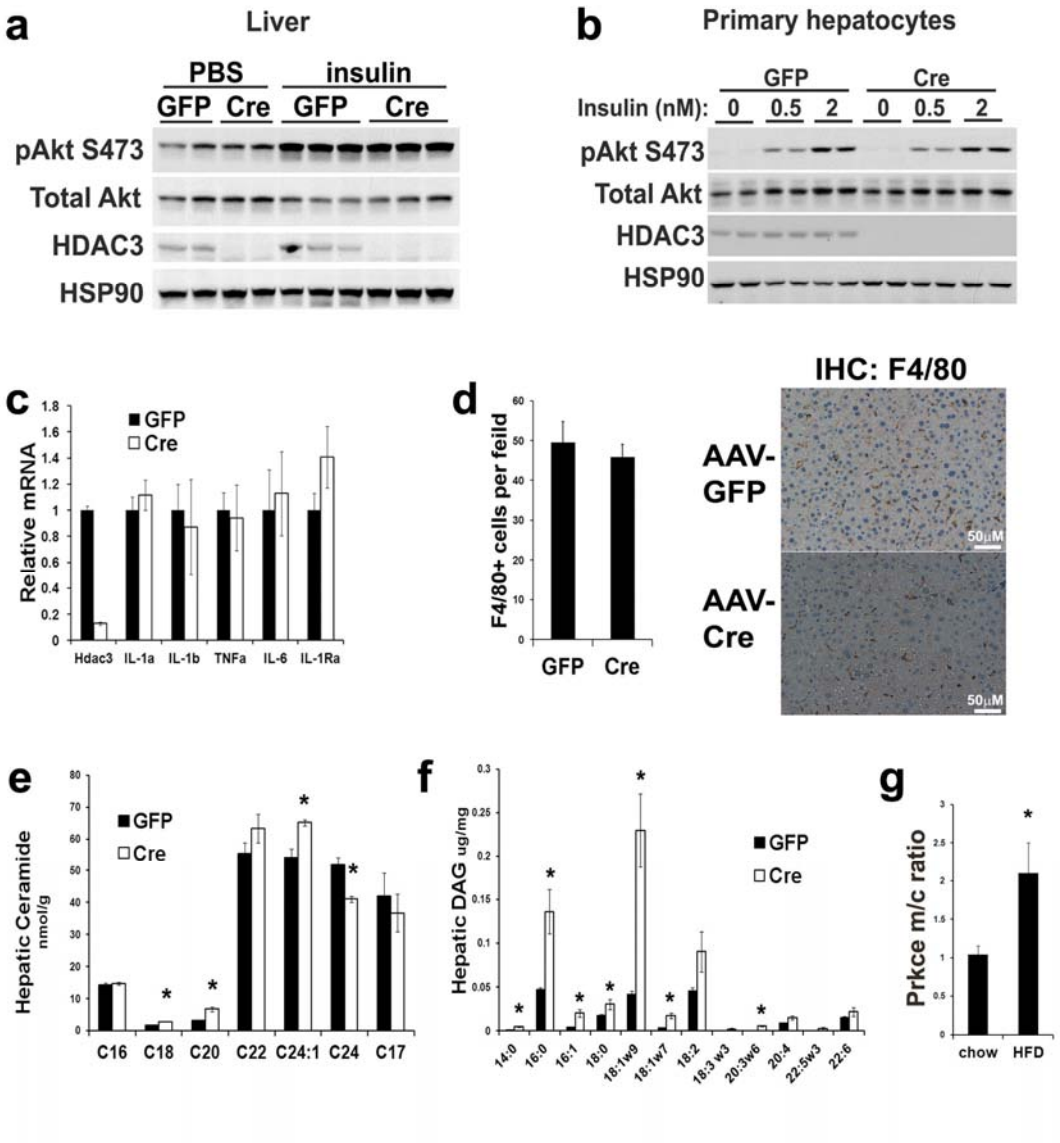

Supplementary Figure 3. Insulin signaling and potential regulators of insulin sensitivity in Hdac3 null livers. (**a**) Western blot analysis of total liver lysates. Overnight fasted mice were i.p. injected with insulin or PBS at 0.5 mU per kg body weight followed by tissue harvest after 20 min. (**b**) Western blot analysis of primary isolated from AAV-injected mice. Cells were serum starved for 2 h followed by treatment with the indicated amount of insulin for 10 min. (**c**) RT-qPCR analysis of inflammatory genes in liver at 2-weeks after AAV injection on chow. $n = 3$. (**d**) Immunohistochemistry analysis with antibodies to Emr1 (α-F4/80) on paraffin liver sections from mice at 2-weeks after AAV injection. F4/80 positive cells were quantified in 20 random microscopy fields under 40× magnification for both GFP and Cre groups with 4–5 mice in each group. (**e**) Hepatic ceramide measured by LC/MS-MS in liver at 2-weeks after AAV injection on chow. $n = 5$. (**f**) Hepatic diacylglycerol (DAG) measured by gas chromatography in liver at 2-weeks after AAV injection on chow. $n = 5$. (**g**) Prkce (PKCε) translocation assay performed in livers harvested from 5-month old wild-type mice after 4 d feeding HFD. Data was presented as membrane/cytosol (m/c) ratio of Prkce, $n = 9$–10. Error bars indicate s.e.m. * $P < 0.05$.

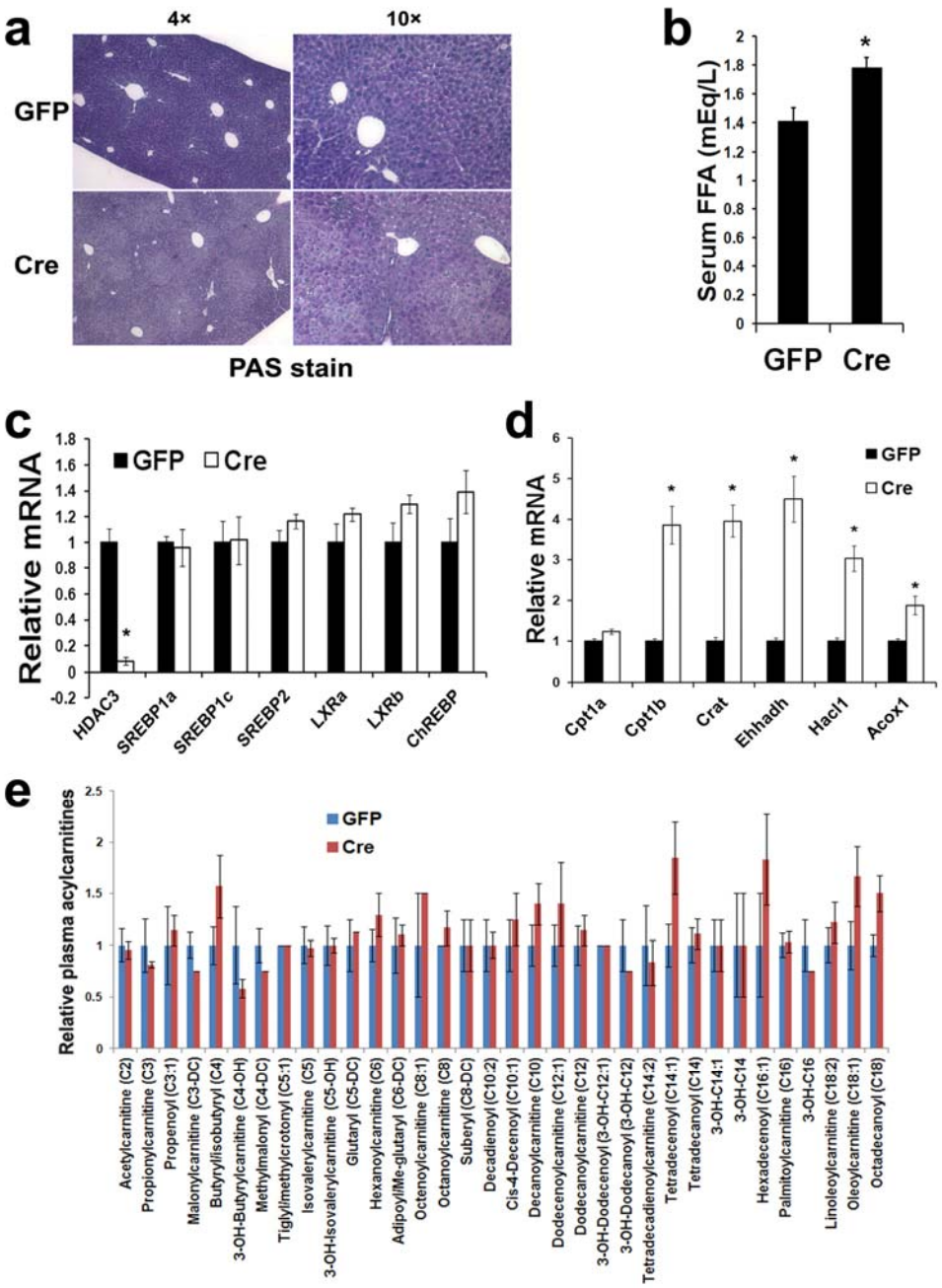

Supplementary Figure 4. Additional characterizations of Hdac3 null liver. (**a**) Periodic acid-Schiff staining of liver at 2-weeks after AAV injection on chow. (**b**) Total free fatty acids (FFA) measurement in serum at 2-weeks since AAV injection and after 12 h fasting, $n = 7–8$. (**c, d**) RT-qPCR analysis of liver at 2-weeks after AAV injection on chow. $n = 5$. (**e**) Plasma acylcarnitine concentrations measured by tandem mass spectrometer from mice at 2-weeks after AAV injection on chow feeding. $n = 3$. Error bars indicate s.e.m. * $P < 0.05$.

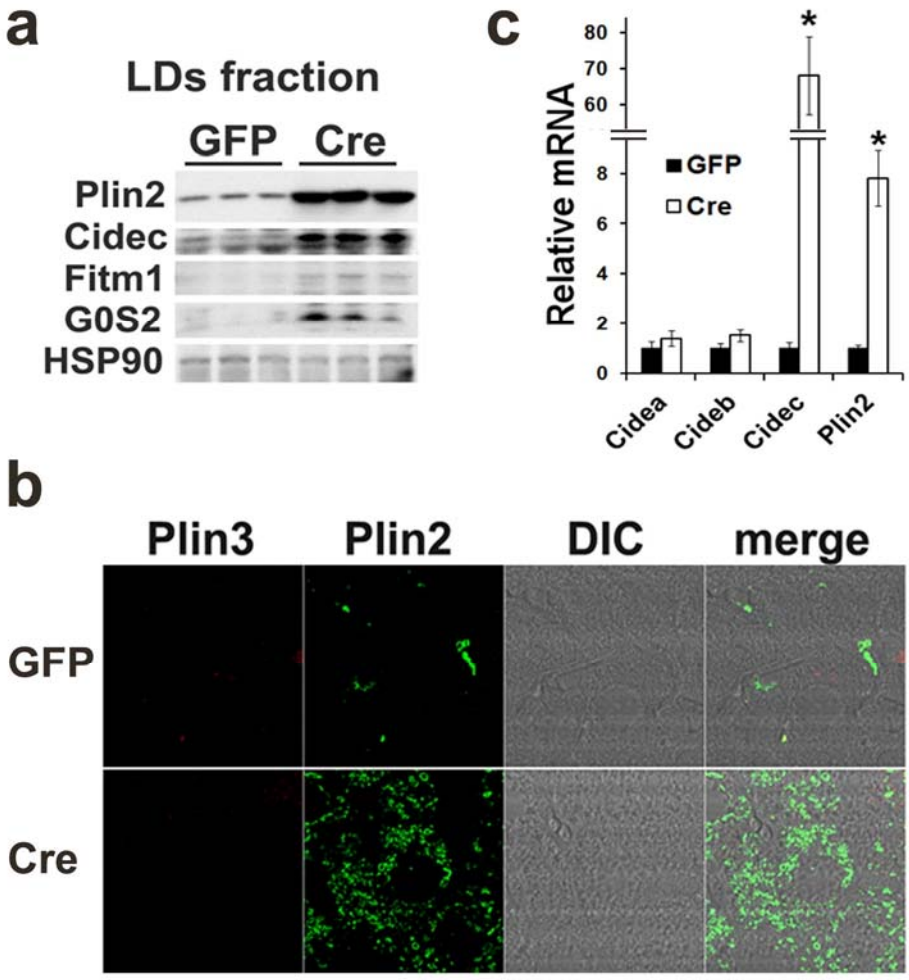

Supplementary Figure 5. Expression of lipid droplet proteins in Hdac3-depleted liver. (**a**) Western blot analysis of lipid droplets (LDs) fractions of liver obtained from AAV-injected mice. LDs fractions were prepared by ultracentrifugation againt 250 mM sucrose. (**b**) Immunofluorescence staining was performed on liver paraffin sections with indicated antibodies. DIC: differential interference contrast. (**c**) RT-qPCR analysis of genes encoding several LDs proteins in liver, $n = 5$. Error bars indicate s.e.m. * $P < 0.05$.

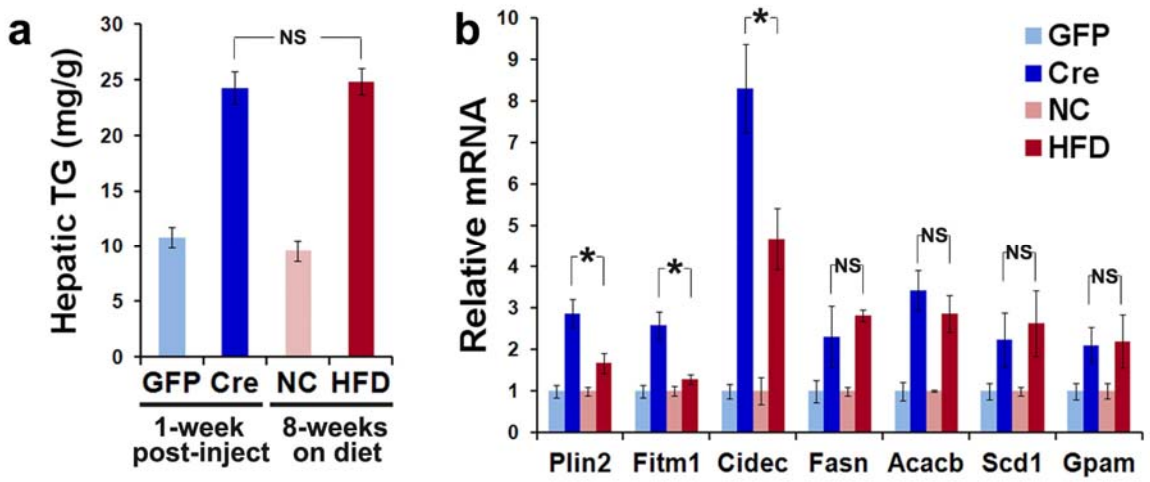

Supplementary Figure 6. **HFD-induced fatty liver displays similar upregulation of genes in lipid synthesis, but much less upregulation of genes involved in lipid sequestration compared to Hdac3-depleted liver at comparable degrees of steatosis.** (**a**) Measurement of hepatic TG accumulation induced by Hdac3 deletion (1-week after AAV injection) and high-fat diet (HFD) feeding (8 weeks). (**b**) RT-qPCR analysis of liver from either mice at 1-week after AAV injection on chow, or wild-type mice fed different diets for 8-weeks. Data were presented as relative units after normalization of the Cre group to the GFP group, and the HFD group to the normal chow (NC) group, respectively. $n = 3$. Error bars indicate s.e.m. * $P < 0.05$. NS: not significant by statistic test.

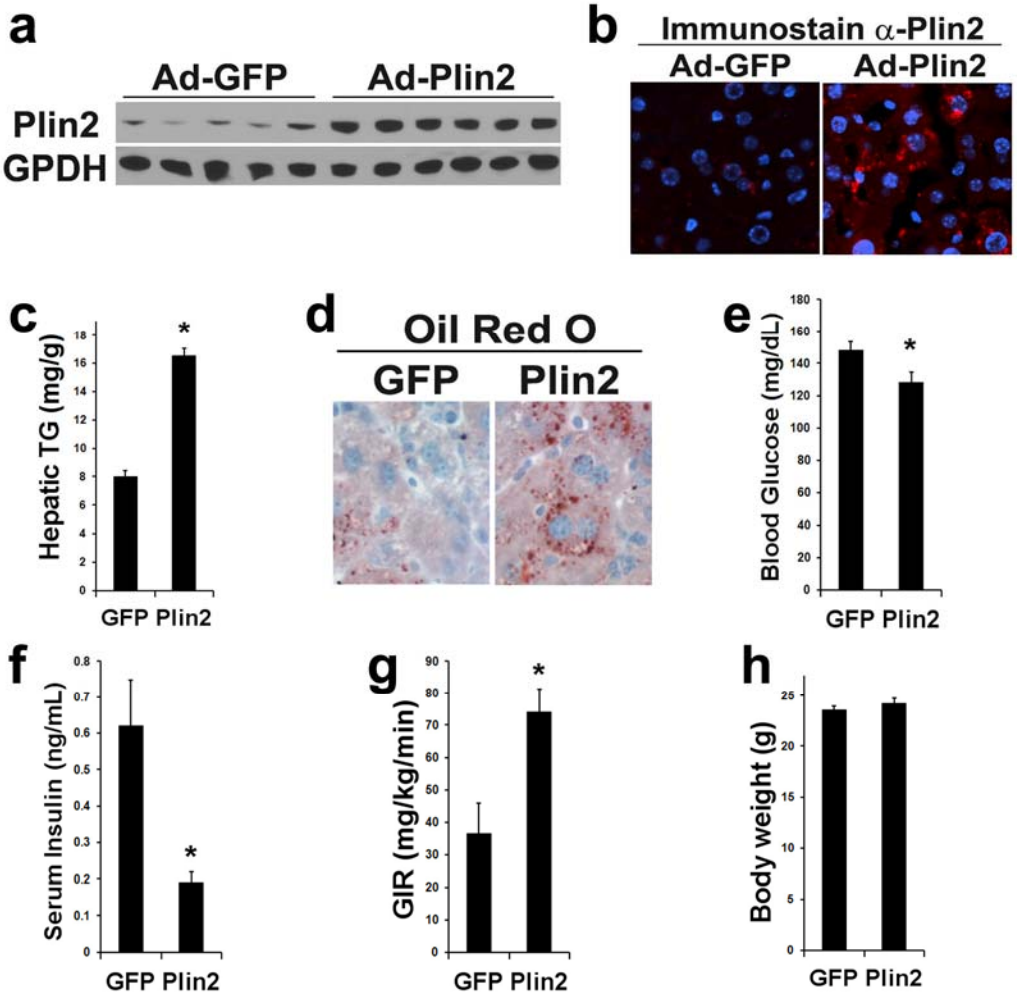

Supplementary Figure 7. Overexpression of Plin2 in liver in wild-type mice results in hepatic steatosis and improved insulin sensitivity. (**a**) Western blot analysis of liver from mice injected with adenovirus (Ad) overexpressing Plin2. (**b**) Immunofluorescence staining of liver paraffin sections with the antibody to Plin2 (α-Plin2). Red indicates Plin2, blue indicates nuclei. (**c**) Hepatic TG measurement, $n = 10$. (**d**) Representative images of Oil Red O staining on liver sections. (**e**) Fasting blood glucose concentrations, $n = 10$. (**f**) Basal serum insulin concentrations, $n = 10$. (**g**) Glucose infusion rate (GIR) obtained from hyperinsulinemic-euglycemic clamp study, $n = 4$. (**h**) Body weight measurement, $n = 10$. All measurements were made at 1-week after virus injection. Error bars indicate s.e.m. * $P < 0.05$.

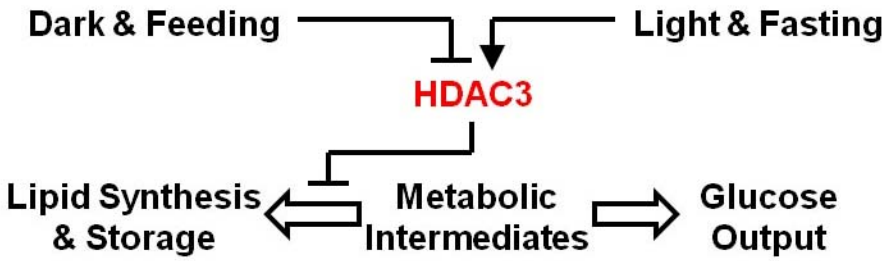

Supplementary Figure S8. Hdac3 controls rhythmic re-routing of metabolic intermediates in normal physiology. A model depicting rhythmic re-routing of metabolic intermediates between lipid synthesis and gluconeogenesis, directly regulated by the molecular circadian clock through the epigenomic modifier Hdac3.